Sulfated Progesterone Metabolites That Enhance Insulin Secretion via TRPM3 Are Reduced in Serum From Women With Gestational Diabetes Mellitus

Hei Man Fan,[1] Alice L. Mitchell,[1] Elena Bellafante,[1] Saraid McIlvride,[1] Laura I. Primicheru,[2] Mirko Giorgi,[3] Ivano Eberini,[4] Argyro Syngelaki,[1] Anita Lövgren-Sandblom,[5] Peter Jones,[1] David McCance,[6] Nithya Sukumar,[7,8] Nishanthi Periyathambi,[7,8] Yonas Weldeselassie,[7,8] Katharine F. Hunt,[1] Kypros H. Nicolaides,[1] David Andersson,[2] Stuart Bevan,[2] Paul T. Seed,[1] Gavin A. Bewick,[1] James E. Bowe,[1] Franca Fraternali,[3] Ponnusamy Saravanan,[7,8] Hanns-Ulrich Marschall,[9] and Catherine Williamson[1]

Diabetes 2022;71:837–852 | https://doi.org/10.2337/db21-0702

Serum progesterone sulfates were evaluated in the etiology of gestational diabetes mellitus (GDM). Serum progesterone sulfates were measured using ultra-performance liquid chromatography–tandem mass spectrometry in four patient cohorts: *1*) the Hyperglycemia and Adverse Pregnancy Outcomes study; *2*) London-based women of mixed ancestry and *3*) U.K.-based women of European ancestry with or without GDM; and *4*) 11–13 weeks pregnant women with BMI ≤25 or BMI ≥35 kg/m^2 with subsequent uncomplicated pregnancies or GDM. Glucose-stimulated insulin secretion (GSIS) was evaluated in response to progesterone sulfates in mouse islets and human islets. Calcium fluorescence was measured in HEK293 cells expressing transient receptor potential cation channel subfamily M member 3 (TRPM3). Computer modeling using Molecular Operating Environment generated three-dimensional structures of TRPM3. Epiallopregnanolone sulfate (PM5S) concentrations were reduced in GDM ($P < 0.05$), in women with higher fasting plasma glucose ($P < 0.010$), and in early pregnancy samples from women who subsequently developed GDM with BMI ≥35 kg/m^2 ($P < 0.05$). In islets, 50 μmol/L PM5S increased GSIS by at least twofold ($P < 0.001$); isosakuranetin (TRPM3 inhibitor) abolished this effect. PM5S increased calcium influx in TRPM3-expressing HEK293 cells. Computer modeling and docking showed identical positioning of PM5S to the natural ligand in TRPM3. PM5S increases GSIS and is reduced in GDM serum. The activation of GSIS by PM5S is mediated by TRPM3 in both mouse and human islets.

Gestational diabetes mellitus (GDM) is characterized by hyperglycemia first occurring or diagnosed during pregnancy. GDM is increasingly prevalent, affecting up to 15% of pregnancies worldwide, with higher rates in Asia (1,2). The pathogenesis of GDM is not fully understood. In addition to maternal hyperglycemia, GDM is also associated with dyslipidemia (3,4) preeclampsia (5), and increased perinatal risks, including large-for-gestational-age infants, birth-related injuries, and neonatal hypoglycemia (6,7). Long-term risks associated with GDM include an increased risk of developing type 2 diabetes and other obesity-related disorders in both mother and offspring (8,9).

[1]School of Life Course Sciences, King's College London, London, U.K.
[2]Wolfson Centre for Age-Related Diseases, Institute of Psychiatry, Psychology and Neuroscience, King's College London, London, U.K.
[3]Randall Division of Cell and Molecular Biophysics, King's College London, London, U.K.
[4]Department of Pharmacological and Biomolecular Sciences, University of Milan La Statale, Milan, Italy
[5]Department of Laboratory Medicine, Karolinska Institute, Stockholm, Sweden
[6]Regional Centre for Endocrinology and Diabetes, Royal Victoria Hospital, Belfast, U.K.
[7]Department of Diabetes, Endocrinology and Metabolism, George Eliot Hospital, Nuneaton, U.K.
[8]Populations, Evidence and Technologies, Division of Health Sciences, Warwick Medical School, University of Warwick, Coventry, U.K.
[9]Department of Molecular and Clinical Medicine/Wallenberg Laboratory, University of Gothenburg, Gothenburg, Sweden

Corresponding author: Catherine Williamson, catherine.williamson@kcl.ac.uk

Received 6 August 2021, and accepted 19 January 2022

This article contains supplementary material online at https://doi.org/10.2337/figshare.18813578.

Serum concentrations of sulfated progesterone metabolites are increased ∼100-fold in the serum of pregnant women compared with nonpregnant women; progesterone sulfates normally circulate at very low concentrations in nonpregnant women and men (10). Some progesterone sulfates bind receptors that influence lipid, glucose, and bile acid metabolism. The progesterone sulfate 5β-pregnan-3α-20α-diol-sulfate (pregnanediol sulfate [PM3S]) activates the G-protein–coupled bile acid receptor 1 (GPBAR1, or TGR5) (11), and 5α-pregnan-3β-ol-20-one-sulfate (epiallopregnanolone sulfate [PM5S]) is a partial agonist for the bile acid receptor farnesoid X receptor (FXR) (10); this may be of relevance to the etiology of GDM, as *Fxr*$^{-/-}$ and *Tgr5*$^{-/-}$ mice have impaired glucose tolerance in pregnancy (12). Another cholesterol-based sulfated endogenous neurosteroid, 5-pregnen-3β-ol-20-one-sulfate (pregnenolone sulfate [PMΔ5S]), is a well-established modulator of receptors and channels such as transient receptor potential cation channel subfamily M member 3 (TRPM3). PMΔ5S has been reported to increase neurotransmitter release and affect synaptic transmission, and, when TRPM3 is activated by PMΔ5S in islets, there is calcium influx and insulin secretion (13–15).

Progesterone sulfates primarily differ between the orientation of the sulfate group on carbon 3 and hydrogen on carbon 5, whether there is a hydroxyl or keto group at carbon 20 position, and whether one or two hydroxyl groups are sulfated. These structural differences alter the predicted conformation of the different progesterone sulfates and are expected to determine their ability to bind to different receptors. Thus, determining whether there are differences in specific progesterone sulfate metabolites between GDM and healthy pregnancy and establishing which receptors these metabolites activate are key to understanding whether progesterone sulfates play a role in the development or progression of GDM.

We hypothesized that specific progesterone sulfates are altered in GDM, and this in turn alters signaling through its receptors, leading to changes in glucose tolerance.

RESEARCH DESIGN AND METHODS

Human Serum Sample Studies

Progesterone sulfates were measured in serum from four separate patient cohorts (Fig. 1 and Table 1).

Cohort 1 comprised 187 fasting samples from the Hyperglycemia and Adverse Pregnancy Outcomes (HAPO) study archive (Belfast, U.K.); progesterone sulfate concentrations were assayed in samples from women in the quartiles with the lowest fasting plasma glucose (FPG) (<4.3 mmol/L; 94 samples) or highest FPG (5.1–6.6 mmol/L; 93 samples) using current International Association of Diabetes and Pregnancy Study Groups criteria. These samples were collected between 2000 and 2006 from women between 24 and 32 weeks' gestation at the Royal Victoria Hospital (Belfast, U.K.). Participants gave written informed consent, with ethical approval obtained from the Northern Ireland Regional Ethics Committee (RO1-HD34242, RO1-HD34243, and RD04/0002756). Methods have been previously published (7).

Cohort 2 comprised samples from Bowe et al. (16) described previously (Research Ethics Committee [REC] number: 13/LO/0539). Due to the availability of the samples, we analyzed fasting serum progesterone sulfate concentrations from 25 women with GDM and 64 without GDM between 26 and 34 weeks' gestation. GDM was diagnosed according to the International Association of Diabetes and Pregnancy Study Groups criteria. Other medical conditions of note that the women had were: in those without GDM, polycystic ovary syndrome (PCOS) (2), hypothyroidism (1), hypertension (1), and asthma (4); and in GDM, PCOS (1) and asthma (4).

Cohort 3 comprised samples collected from the micronutrients in the Pregnancy as a Risk Factor for gestational Diabetes and Effects on mother and baby (PRiDE) study, carried out in 10 sites (Midlands, Leeds, and York, U.K.), methods previously published (REC number 12/WM/0010) (17). We used fasting samples of European origin only, collected from 2013–2018, and with a diagnosis of GDM using a modified National Institute for Health and Care Excellence 2015 criteria (FPG ≥5.6 mmol/L and/or 2-h plasma glucose ≥7.8 mmol/L). Samples were further split by BMI, being classified as normal BMI (<25 kg/m^2) or obese BMI (>30 kg/m^2).

Cohort 4 comprised samples collected at 11–13 weeks' gestation, between 2010 and 2015 at King's College Hospital (London, U.K.). Invited participants gave written informed consent; the study was approved by the National REC (REC number 02–03–033). Serum samples were collected in women attending for their routine first trimester ultrasound scan and stored at −80°C for subsequent biochemical analysis. Screening for GDM in the hospital was based on a two-step approach. A random plasma glucose was measured in all women at 24–28 weeks' gestation. If the concentration of glucose was ≥6.7mmol/L, an oral glucose tolerance test was performed within the subsequent 2 weeks. Diagnosis of GDM was made if FPG level was ≥6 mmol/L or ≥7.8 mmol/L after 2 h. Progesterone sulfate concentrations were measured in 11–13 weeks' serum samples from 100 women who subsequently developed GDM and 100 women who had an uncomplicated pregnancy, defined as pregnancies occurring without complications that resulted in live birth after 37 weeks' gestation of phenotypically normal neonates. GDM samples were selected according to maternal BMI at 11–13 weeks' gestation; 50 samples per group from women with BMI ≤25 kg/m^2 or with BMI ≥35 kg/m^2. Each GDM sample was matched to one uncomplicated pregnancy sample for the BMI group, with samples taken on the same or next day. Other medical conditions of note that the women had were: in those without GDM, PCOS (4), hypothyroidism (3), hyperthyroidism (1), hypertension (2), and asthma (6); and in

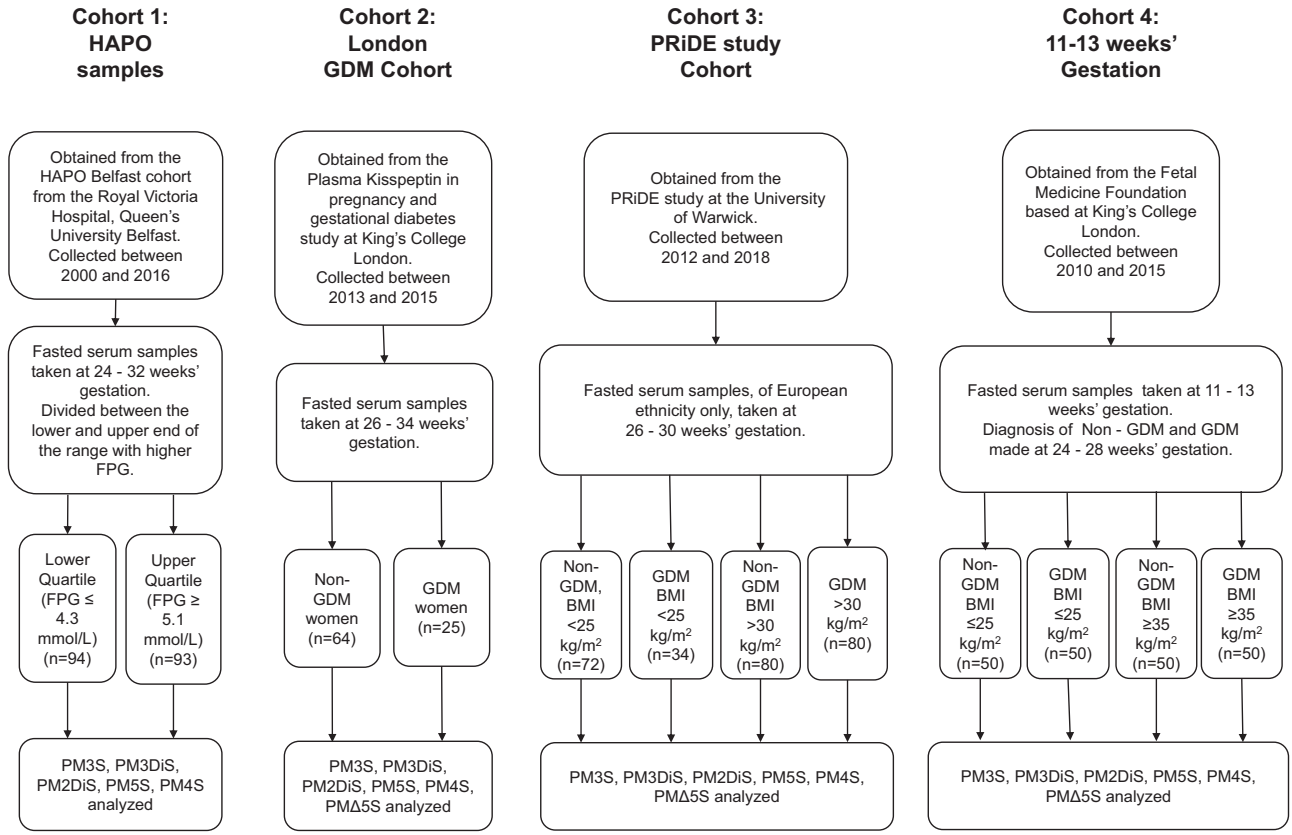

Figure 1—Flow chart detailing each of the cohorts of the study.

GDM, PCOS (5), hypothyroidism (3), hyperthyroidism (1), hypertension (3), and asthma (4).

No participants in any cohort had a diagnosis of intrahepatic cholestasis of pregnancy, a condition known to be associated with elevated serum progesterone sulfate concentrations.

Serum Progesterone Sulfate Analysis by Ultra-Performance Liquid Chromatography–Tandem Mass Spectrometry

Serum samples were analyzed for progesterone sulfates in all four cohorts by ultra-performance liquid chromatography–tandem mass spectrometry (UPLC-MS/MS) as previously described (11). It was not possible to assay PMΔ5S in the HAPO samples, as these samples were analyzed before the D4-labeled internal standard for unsaturated progesterone metabolites became available in 2018. Assays were performed in the Department of Laboratory Medicine, Karolinska Institute (Stockholm, Sweden).

Animals

Female 8–10-week-old virgin C57Bl/6J wild-type (WT) mice purchased from Charles River Laboratories (Tranent, U.K.) were used for islet studies. *Fxr*$^{-/-}$ and *Tgr5*$^{-/-}$ female 8–10-week-old virgin mice used for islet studies were maintained on a C57BL/6J background and have been previously described in detail (18,19). Mice were housed in stable conditions with a 12-h light/dark cycle.

Islet Studies

Female mouse islets were isolated by collagenase digestion (1 mg/mL) of the pancreas and separated from exocrine pancreatic tissue on a Histopaque gradient. Islets were incubated at 37°C in RPMI 1640 (10% FBS, 2 mmol/L glutamine, 100 units/mL penicillin/0.1 mg/mL streptomycin, and 11 mmol/L glucose) overnight before experiments were performed.

Human islets were isolated from female organ donors at the King's College Hospital Islet Transplantation unit, as previously described (20). Consent for using islets for research has been obtained and studies approved by the Ethical committee of King's College Hospital (REC number: LREC 01–082). Islets were isolated between 2018 and 2019. Islets isolated from four donor pancreases were received within 48 h of pancreas harvest. Supplementary Table 1 details the age, sex, and BMI of each organ donor.

Glucose-stimulated insulin secretion (GSIS) from islets was assessed in static incubations. Islets were preincubated in 2 mmol/L glucose RPMI. Groups of five size-matched islets were then incubated for 1 h at 37°C in a bicarbonate-buffered physiological salt solution, supplemented with 2 mmol/L $CaCl_2$, 0.5 mg/mL BSA, and either low glucose

Table 1—Clinical and demographic characteristics of each patient cohort

	HAPO fasting samples (cohort 1)		London GDM study (cohort 2)		PRiDE study (cohort 3)			
	FPG ≤4.3 mmol/L	FPG ≥5.1 mmol/L	Control subjects	GDM	Without GDM, normal BMI <25 kg/m^2	Without GDM, obese BMI >30 kg/m^2	With GDM, normal BMI <25 kg/m^2	With GDM, obese BMI >30 kg/m^2
Number of participants	94	93	64	25	72	80	34	80
Maternal age (years), median (range)	29.1 (25.4–33.6)	31.9 (29–34.9)	33 (30.8–38)	33 (31–36)	29.3 (25.8–34.8)	28.9 (26.3–32)	34.2 (30.9–36.3)	30.9 (28.3–35.4)
Gestational age of sample (weeks), median (range)	29.1 (28.5–29.7)	29.1 (28.6–29.7)	29 (28–30)	29 (28–30)	27.4 (26.9–28.2)	27.6 (26.6–28.3)	26.7 (25.7–27.9)	26.6 (26.1–27.6)
Ethnicity, *n* (%)								
White	94 (100)	93 (100)	35 (54.7)	14 (56)	72 (100)	80 (100)	34 (100)	80 (100)
Black	0 (0)	0 (0)	17 (26.6)	6 (24)	0 (0)	0 (0)	0 (0)	0 (0)
Asian	0 (0)	0 (0)	5 (7.8)	2 (8)	0 (0)	0 (0)	0 (0)	0 (0)
Mixed	0 (0)	0 (0)	3 (4.7)	2 (8)	0 (0)	0 (0)	0 (0)	0 (0)
Other	0 (0)	0 (0)	4 (6.3)	1 (4)	0 (0)	0 (0)	0 (0)	0 (0)
BMI (kg/m^2), median (range)	21.7 (20.3–23.6)	25.6 (23.1–32.8)	28.7 (25.3–33.7)	31.6 (26.8–35.6)	19.7 (18.7–22.7)	46.4 (37.1–50.3)	23.1 (21.3–24.3)	42.5 (40.5–44.1)
Singleton pregnancies, *n* (%)	—	—	62 (96.9)	25 (100)	72 (100)	79 (98.8)	34 (100)	80 (100)
Parity (nulliparous vs. multiparous)	—	—	22 vs. 42	6 vs. 19	53 vs. 19	65 vs. 15	26 vs. 8	61 vs. 19
Previous GDM, *n* (%)	—	—	41 (64.1)	17 (68)	5 (6.9)	0 (0)	13 (38.2)	5 (6.3)
Blood glucose (mmol/L), median (range)								
0 min	4.2 (4.1–4.3)	5.2 (5.1–5.5)	4.3 (4.2–4.6)	4.8 (4.5–5.3)	4.3 (4.1–4.5)	4.5 (4.3–4.8)	4.7 (4.2–5.2)	5.3 (5.1–5.7)
60 min	6.6 (5.6–7.9)	8.7 (7.7–9.8)	7.6 (6.7–8.6)	9.9 (8.6–10.2)	—	—	—	—
120 min	5.5 (4.9–6.3)	6.8 (5.9–8.2)	6.6 (5.8–7.2)	8.6 (8.1–9.1)	5.2 (4.5–6.2)	5.6 (5.1–6.7)	8.5 (6.5–9.3)	7.0 (5.9–8.7)

	Early Pregnancy Study (cohort 4)			
	Control BMI ≤25 kg/m^2	GDM BMI ≤25 kg/m^2	Control BMI ≥35 kg/m^2	GDM BMI ≥35 kg/m^2
Number of participants	50	50	50	50
Maternal age (years), median (range)	32.8 (29.3–34.5)	33.1 (30.2–37.5)	29.3 (26–34.1)	32.8 (29.6–36.1)
Gestational age of sample (weeks), median (range)	12.6 (12.1–13)	12.5 (12–13)	12.7 (12.2–13)	12.7 (12.3–13.1)
Ethnicity, *n* (%)				
White	40 (80)	30 (60)	27 (54)	17 (34)
Black	6 (12)	5 (10)	20 (40)	30 (60)
Asian	2 (4)	13 (26)	1 (2)	2 (4)
Mixed	2 (4)	2 (4)	2 (4)	1 (2)
Other	0 (0)	0 (0)	0 (0)	0 (0)

Continued on p. 841

Table 1—Continued

	Early Pregnancy Study (cohort 4)			
	Control BMI ≤25 kg/m^2	GDM BMI ≤25 kg/m^2	Control BMI ≥35 kg/m^2	GDM BMI ≥35 kg/m^2
BMI (kg/m^2), median (range)	22.1 (21.3–23.4)	22.3 (21–23.7)	37.5 (35.9–38.6)	37.9 (36.3–40.8)
Singleton pregnancies	—	—	—	—
Parity (nulliparous vs. multiparous)	24 vs. 26	27 vs. 23	21 vs. 29	11 vs. 39
Previous GDM, *n* (%)	—	12 (52)	—	16 (41)

— indicates no data gathered for that cohort.

(2 or 3 mmol/L) or high glucose (20 mmol/L), with the agents of interest. Incubation medium was collected and stored at −20°C until assayed. Insulin content from the collected medium from all static incubations was determined using an in-house radioimmunoassay as described previously (21), apart from *Fxr*$^{-/-}$ islet experiments, which were determined by ELISA (62IN2PEG; Cisbio, Bedford, MA).

Cell Culture

HEK293 cells (RRID: CVCL_U427; Thermo Fisher Scientific, Horsham, U.K.) stably expressing TRPM3α2 plasmid (pcDNA3.1) DNA (provided by Dr. Stephan Philipp, University of Saarland, Homburg, Germany) were grown in DMEM AQ supplemented with penicillin (100 U/ml), streptomycin (100 μg/mL), FBS (10%), and G418 (0.5 mg/mL).

Ninety-Six–Well Plate Intracellular Calcium Concentration Assays

HEK293 cells expressing TRPM3 were plated in poly-D-lysine–coated 96-well black-walled plates (Costar; Corning, Corning, NY) 1 day before experimentation. Cells were loaded with 2.5 μmol/L Fura-2 AM (Invitrogen, Paisley, U.K.) in the presence of 1 mmol/L of probenecid (Tocris Bioscience, Bristol, U.K.) for ∼1 h. Dye loading and all experiments were performed in a physiological saline solution containing 140 mmol/L NaCl, 5 mmol/L KCl, 10 mmol/L glucose, 10 mmol/L HEPES, 2 mmol/L $CaCl_2$, and 1 mmol/L $MgCl_2$, buffered to pH 7.4 (NaOH). Progesterone sulfate solutions were injected and responses read using the FlexStation 3 Multi-Mode Microplate Reader (Molecular Devices) at 37°C. Basal emission ratios (340 nm/380 nm) were measured and then changes in dye emission ratio determined at various times after compound addition. Experiments were performed in triplicate wells.

Homology Modeling and Ligand Binding Modeling

Molecular Operating Environment (MOE) version 2019.01 was used to visualize the binding sites and superimpose and dock the structures of PMΔ5S and PM5S.

The model of human TRPM3 was built through the "Homology model" program of the "Protein" module of the MOE by Chemical Computing Group ULC (https://www.chemcomp.com).

UniProt was used to retrieve the primary structure of human TRPM3 and to run a protein BLAST search of the Protein Data Bank database to identify a suitable homologous template. Mouse TRPM7 (Protein Data Bank identification number 5ZX5) (22) was identified as the top-scoring template for comparative modeling.

Human TRPM3 and mouse TRPM7 primary structures were globally aligned with the "Align/Superpose" program of the MOE "Protein" module and manually improved, taking into account also the alignment produced by Schrödinger

(https://schrodinger.com) BioLuminate alignment tools contained in the "Multiple Sequence View/Editor."

Ten different intermediate models were produced, and the top-scoring one, according to the electrostatic solvation energy, calculated used a Generalized Born/Volume Integral (GB/VI) methodology (23), was selected and energy-minimized.

Since mouse TRPM7 was cocrystallized and solved with several cholesterol hemisuccinate molecules that share the same cyclopentanoperhydrophenanthrene scaffold of our investigated ligands, we transferred them in our final human TRPM3 model, using the MOE "Homology model" option "Used as environment."

Molecular docking was carried out on the refined human TRPM7 using the MOE "Dock" program of the "Compute" module, testing a database containing the progesterone sulfates PMΔ5S and PM5S. The three different cholesterol hemisuccinate binding sites were sequentially tested, with the following settings: placement "Triangle Matcher," score "London ΔG," number of retained poses per ligand "30," refinement "Rigid Receptor," score "GB/VI/WSA ΔG," and number of retained poses per ligand "5." Both of the empirical scoring functions, the London ΔG and the GB/VI/WSA ΔG (24), used for scoring the produced docking poses are expressed as kilocalories per mole and estimated an approximate binding free energy value for each generated complex.

Three-Dimensional Structures of Progesterone Sulfates

MM2 energy minimization modeling using ChemDraw 3D (PerkinElmer) was used to create the three-dimensional (3D) structures of progesterone sulfates.

Materials

All drugs and reagents were purchased from Sigma-Aldrich (Gillingham, U.K.) unless otherwise stated. The source of progesterone sulfates was Steraloids (Newport, RI); isosakuranetin (ISO) was purchased from Extrasynthese (Genay, France).

Statistical Analysis

Data are expressed as mean ± SEM. Normality of data was tested using the Shapiro-Wilk test; if not normally distributed, the data were transformed using the logarithmic function. Where two groups were being compared, Student *t* test or a Mann-Whitney test was used. When three or more groups were compared, a one-way ANOVA was used followed by Tukey post hoc analysis or a Kruskal-Wallis test followed by a Dunn post hoc test. Spearman rank correlation coefficient was used to evaluate the strength of two variables in the data. A P value of <0.05 was considered significant. All statistical analyses were made using Prism version 8.4.2 (GraphPad Software). Logistic regressions were performed using Stata 16.

Data and Resource Availability

All data generated or analyzed during this study are included in the published article (and its Supplementary Material).

RESULTS

Progesterone Sulfates Are Reduced in GDM

We studied women with FPG concentrations in the highest and lowest quartiles from the HAPO study (cohort 1). Women with higher FPG (5.1–6.6 mmol/L) had significantly lower serum concentrations of PM3S (P = 0.0268), pregnanediol disulfate (P = 0.0186), PM5S (P = 0.0012), and allopregnanolone sulfate (PM4S) (P = 0.0051) in comparison with the women with lower FPG levels (≤4.3 mmol/L) (Fig. 2*A*). We then screened serum samples from London-based women of mixed ancestry with GDM compared with those with normal glucose tolerance (cohort 2) and demonstrated a 1.6- (P = 0.0475) and 1.35-fold (P = 0.0104) decrease in PM5S and PMΔ5S, respectively, in the serum from women with GDM (Fig. 2*B*), consistent with the findings of low serum concentrations of progesterone sulfates in fasted serum from women in cohort 1. There was a negative correlation between maternal BMI and concentrations of PM5S (ρ −0.26; P = 0.017), PM4S (ρ −0.27; P = 0.011), PMΔ5S (ρ −0.22; P = 0.041), and PM3S (ρ −0.42; P = 0.002) in women from this cohort (Supplementary Table 2).

Following the observation of an inverse correlation with BMI, we analyzed serum progesterone sulfates in a second GDM study (PRiDE study, cohort 3), that was collected from U.K.-based women of European ancestry in the third trimester with either obese (>30 kg/m^2) or normal (<25 kg/m^2) BMI. Women with both obese and normal BMI with GDM showed a 1.4- (P = 0.0258) and 1.7-fold (P = 0.0004) decrease in PM5S, respectively, compared with women without GDM (Fig. 2*C* and *D*). Obese women with GDM also demonstrated a 1.3-fold (P = 0.0241) decrease in PM3S compared with obese women without GDM (Fig. 2*D*). FPG concentrations showed significant negative correlations with PM3S (−0.254, $P < 0.0001$), PM5S (−0.333; $P < 0.0001$), and PM4S (−0.239; $P < 0.0001$) in cohort 3 when analyzing the whole cohort (i.e., women of European ancestry with and without GDM). However, when the comparison was performed using only data from women with GDM, no significance was seen (Supplementary Table 3). This may relate to a continuum of risk for elevated FPG related to reduced progesterone sulfate concentrations in women with GDM of European ancestry.

To establish whether progesterone sulfate concentrations are also reduced in early pregnancy in women who subsequently develop GDM and whether BMI influences this reduction, we studied early pregnancy samples from women who attended for serum screening at 11–13 weeks' gestation (cohort 4), segregating samples from women with lower or higher BMI. Women with a normal

A

Cohort 1: HAPO fasting samples

Progesterone sulfate	FPG ≤ 4.3 mmol/L	FPG ≥ 5.1 mmol/L	Significant
PM3S, mean ± SD	2.13 ± 2.35	1.44 ± 1.82	P=0.0268
PM3DiS, mean ± SD	2.17 ± 1.09	1.81 ± 0.97	P=0.0186
PM2DiS, mean ± SD	1.94 ± 2.27	1.46 ± 1.95	NS
PM5S, mean ± SD	5.12 ± 6.28	2.62 ± 3.79	P=0.0012
PM4S, mean ± SD	1.13 ± 1.43	0.63 ± 0.90	P=0.0051

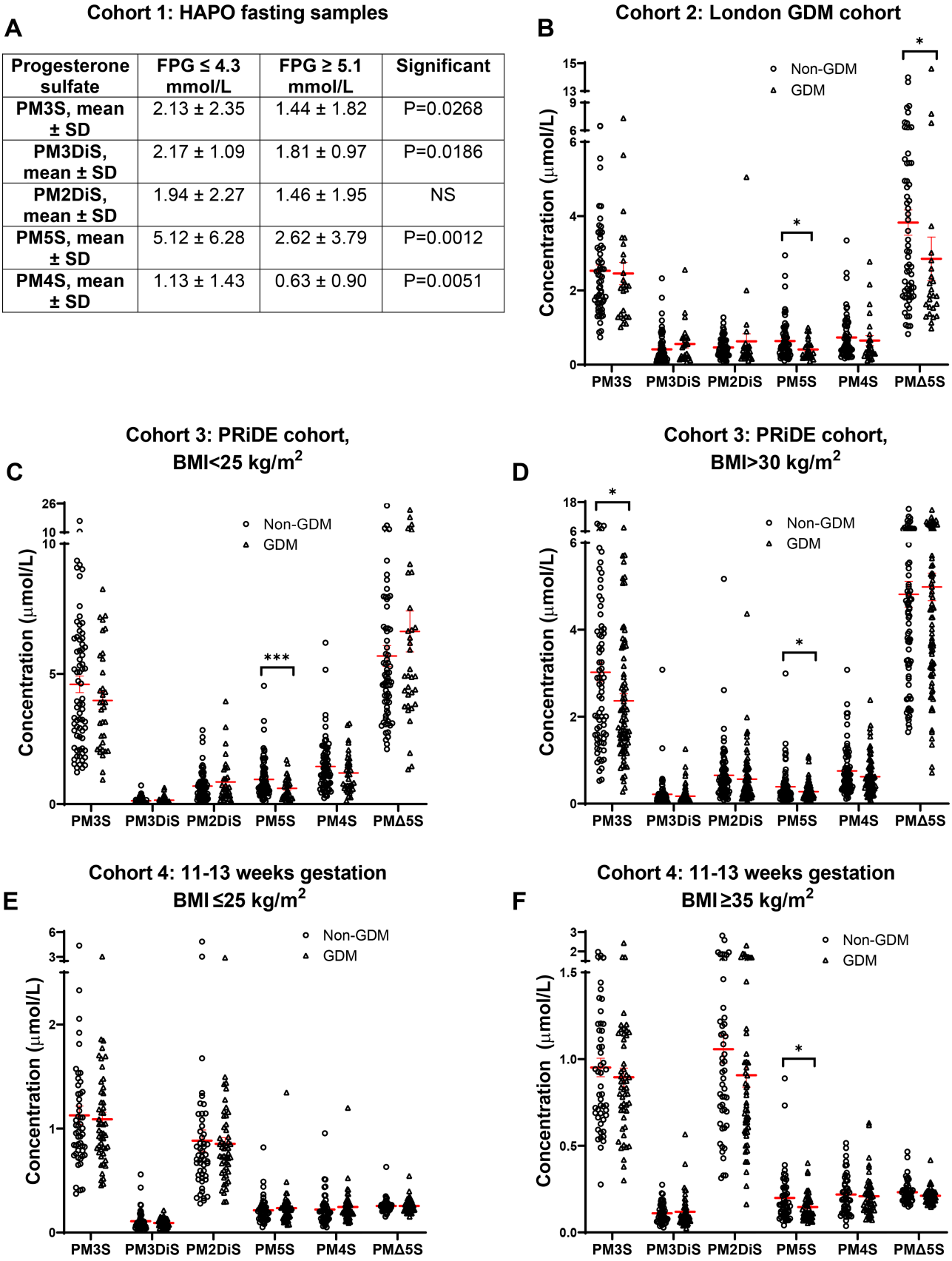

Figure 2—Progesterone sulfates are reduced in GDM. Serum samples from four patient cohorts were assayed using UPLC-MS/MS for abundances of different progesterone sulfates: PM3S, pregnanediol disulfate (PM3DiS), allopregnanediol disulfate (PM2DiS), PM5S,

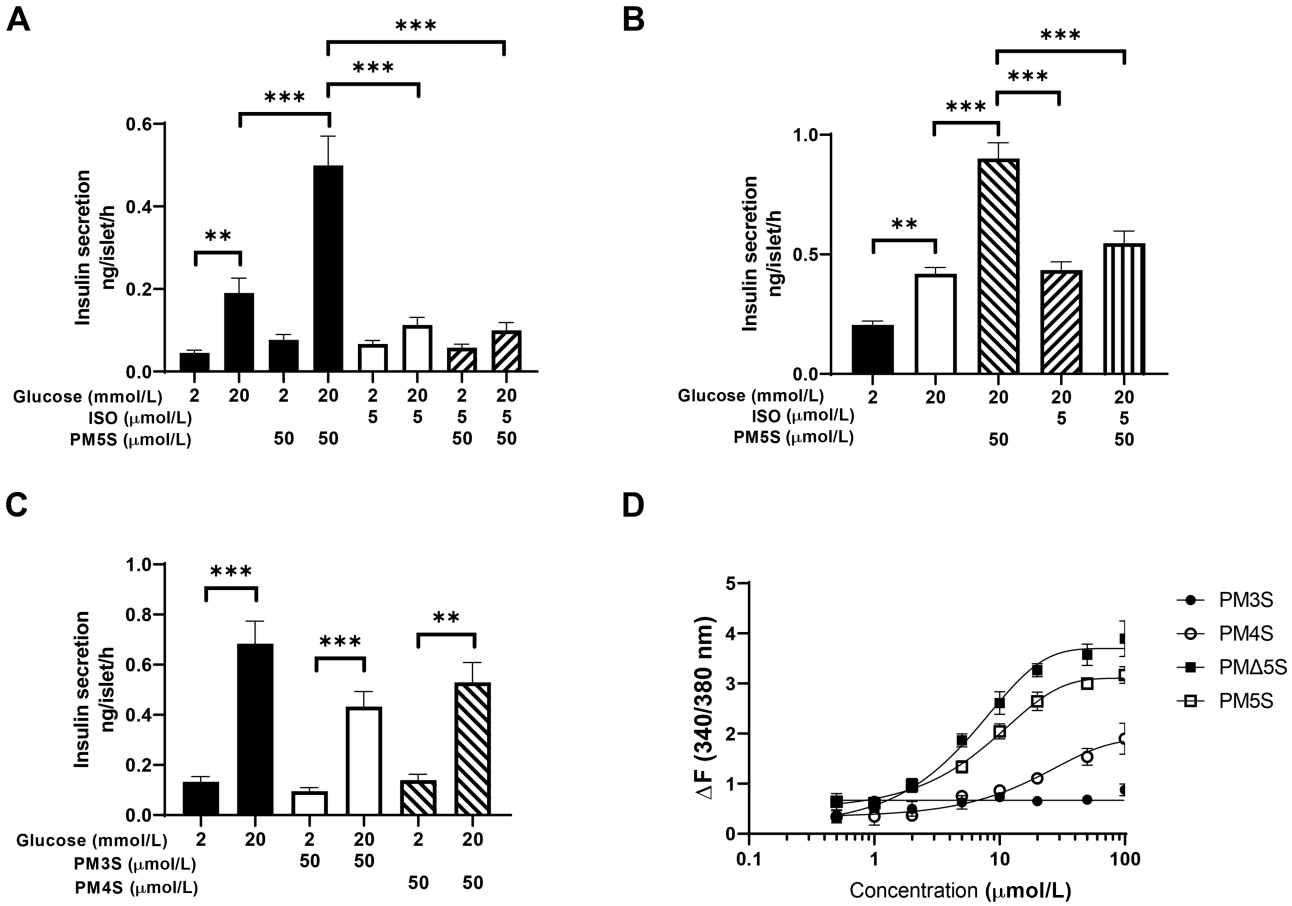

Figure 3—PM5S increases GSIS in murine and human islets via TRPM3. Insulin secretion in response to incubation with PM5S was assessed in islets from mice or humans at low (2 mmol/L) and high (20 mmol/L) concentrations of glucose. *A*: WT mouse islets were incubated with the TRPM3 antagonist ISO and/or PM5S. *B*: Human islets were similarly incubated with ISO and/or PM5S at high glucose concentrations. *C*: WT mouse islets were incubated with either PM3S or PM4S at low and high glucose concentrations. *D*: HEK cells transfected with TRPM3 were loaded with Fura-2 to measure changes in intracellular calcium concentration. Increasing concentrations of progesterone sulfates were given. Curves are representative examples of each data set. Unless indicated differences between groups were not significant, significance differences are indicated by: $^{**}P < 0.01$, $^{***}P < 0.001$, as determined by one-way ANOVA followed by Tukey multiple-comparisons test or Kruskal-Wallis test followed by Dunn multiple-comparisons test. Data expressed as mean ± SEM; for each graph, n = 3–6 independent experiments, and each group contained five size-matched islets.

BMI who went on to develop GDM showed no difference in progesterone sulfate levels compared with women with a comparable BMI who had uncomplicated pregnancies (Fig. 2*E*). In the high BMI group, however, PM5S was reduced in early pregnancy in women who subsequently developed GDM compared with those who did not (P = 0.0340) (Fig. 2*F*). Thus, high BMI in early pregnancy is associated with reduced serum PM5S in women who subsequently develop GDM, and this lower serum PM5S concentration is maintained in late pregnancy, alongside a decrease in serum PMΔ5S.

Logistic regression was performed to determine whether PM3S or PM5S could predict GDM using the data from cohort 4. While we found a significant difference in PM5S concentrations in the high BMI group, the area under the receiver operating characteristic curve was 0.6, suggesting that it is not a strong predictive biomarker for GDM (Supplementary Table 4).

PM4S, and PMΔ5S. *A*: Serum samples from the HAPO study show reduced progesterone sulfate concentrations (in μmol/L) in women with high FPG (n = 93) compared to low FPG (n = 94). *B*: Serum samples from London-based, mixed-ethnicity women with GDM (n = 25) and control subjects (n = 64). A second U.K. third trimester cohort with GDM (PRiDE study) was examined from women of European ancestry with a normal BMI <25 kg/m^2 without GDM (n = 72) and with GDM (n = 34) (*C*) and with an obese BMI >30 kg/m^2 without GDM and with GDM (n = 80) (*D*). The early pregnancy cohort comprised 11–13-week serum samples separated according to whether they subsequently developed GDM or had uncomplicated pregnancies: women with BMI ≤25 kg/m^2 (*E*) and women with BMI ≥35 kg/m^2 (*F*) (n = 50/group). Significant differences are indicated by: $^{*}P < 0.05$, $^{***}P < 0.001$, as determined by multiple t tests; if data were not normally distributed, Mann-Whitney U tests were performed. Data are expressed as mean ± SD.

Table 2—Names, structures, and approximate calcium responses of each progesterone sulfate investigated

Progesterone sulfate	Ref. for structure*	EC_{50} (μmol/L)	B_{max} (ΔF)	Average maximal response (ΔF)	Predictive response in normal pregnancy (ΔF)	Predictive response in GDM pregnancy (ΔF)
PMΔ5S, Pregnenolone sulfate, 5-pregnen-3β-ol-20-one-sulfate	13, 15	6.2	3.9	3.5	1.5	0.8
PM5S, epiallopregnanolone sulfate, 5α-pregnan-3β-ol-20-one-sulfate	10	7.8	3.3	3.2	1.1–1.6	0.6–1.0
PM4S, allopregnanolone sulfate, 5α-pregnan-3α-ol-20-one-sulfate	10	11.7	—	2.0	0.7–0.9	0.4–0.7
PM3S, pregnanediol sulfate, 5β-pregnan-3α,-20α-diol-3-sulfate	11	—	—	—	—	—

*Structure of PMΔ5S can be found in Drews et al. (13) and Theil et al. (15); PM5S and PM4S can be found in Abu-Hayyeh et al. (10); PM3S can be found in Abu-Hayyeh et al. (11). Predictive responses refer to the ΔF values obtained according to the mean concentrations in Fig. 2. Orientation of sulfate group and of the hydrogen group on carbon number 5 in the first carbon ring affects the 3D orientation of each progesterone sulfate. PM4S are approximate values, as a full dose response could not be determined. — indicates that no response values could be obtained from the experiments.

PM5S Increases GSIS in Murine and Human Islets via TRPM3

Since serum PM5S concentrations are significantly reduced in both early pregnancy prior to GDM diagnosis of women with high BMI and women in late pregnancy who had GDM, we investigated whether PM5S altered islet insulin secretion.

Challenging WT mouse islets with high glucose (20 mmol/L) increased GSIS by 4.2-fold (Fig. 3*A*). While addition of 50 μmol/L PM5S did not affect GSIS under low glucose (2 mmol/L) concentrations, there was a 2.6-fold increase in GSIS when combined with high glucose compared with high glucose concentrations alone, suggesting that PM5S augments insulin release in response to elevated glucose concentrations. The bile acid receptors TGR5 and FXR can bind progesterone sulfates (10,11), and both are expressed in pancreatic β-cells (25). However, when islets from WT, *Tgr5*$^{-/-}$, and *Fxr*$^{-/-}$ were treated with PM5S, no differences in GSIS were observed compared with WT islets (Supplementary Fig. 1).

The ion channel TRPM3 is activated by the progesterone sulfate PMΔ5S (13). As PM5S has similar key orientations and 3D structure to PMΔ5S with a similar 3D structure, we investigated whether PM5S binding to TRPM3 was responsible for increasing GSIS at high glucose concentrations. Mouse and human female islets were coincubated with PM5S with or without the TRPM3 receptor antagonist ISO. Incubation of mouse islets with 5 μmol/L ISO did not alter GSIS at low glucose concentrations, but blunted GSIS in response to high glucose concentrations. Coincubation of ISO with PM5S abolished the previously observed PM5S-augmented GSIS at high glucose concentrations (Fig. 3*A*). In human islets, a twofold elevation in GSIS was observed at high glucose concentrations compared with low glucose, which was further increased by 2.2-fold with PM5S incubation. ISO alone did not alter GSIS at high glucose concentrations but abolished the PM5S-induced increase in GSIS (Fig. 3*B*). Thus, inhibition of the TRPM3 channel by ISO prevents PM5S-stimulated increase in GSIS in response to high glucose levels in both mouse and human female islets.

WT mouse islets were challenged with PM3S and PM4S to determine if these progesterone sulfates changed GSIS. While a 20 mmol/L high glucose challenge increased GSIS by fivefold compared with 2 mmol/L glucose, addition of either 50 μmol/L PM3S or PM4S did not augment GSIS compared with 20 mmol/L glucose alone (Fig. 3*C*).

Cellular Ca^{2+} Concentration Is Increased by Specific Progesterone Sulfates

TRPM3 is a calcium ion channel, and therefore, we assessed changes in intracellular calcium concentrations in response to different progesterone sulfate metabolites using TRPM3-expressing HEK293 cells loaded with the fluorescent calcium indicator dye Fura-2. Addition of PMΔ5S, which is reduced in the serum of women with GDM (Fig. 2*B*) and is an established agonist of TRPM3 (14), caused a concentration-dependent increase of intracellular calcium that began to plateau at 20 μmol/L (half-maximal effective concentration [EC_{50}] value = 6.2 μmol/L; B_{max} = 3.9 ΔF [B_{max} is the maximum specific binding capacity, in the same units as the *y*-axis]) (Fig. 3*D*, Table 2, and Supplementary Fig. 2*A*). PM5S caused a similar concentration-dependent increase of calcium, with a comparable concentration-response curve (EC_{50} = 7.8 μmol/L; B_{max} = 3.3 ΔF [B_{max} is the maximum specific binding capacity, in the same units as the *y*-axis]), which reached maximal effect at 20 μmol/L (Fig. 3*D*, Table 2, and Supplementary Fig. 2*B*). When cells were incubated with PM3S, no increase in calcium concentrations were seen at any concentration (Fig. 3*D* and Supplementary Fig. 2*C*). PM4S showed partial agonism, with an approximate EC_{50} value of 11.7 μmol/L (Fig. 3*D* and Supplementary Fig. 2*D*)

and an average maximal ΔF value at 100 μmol/L of 2 (Table 2). PM4S began to increase intracellular calcium concentration at ∼10 μmol/L but did not evoke the same magnitude of calcium response as seen with PM5S or PMΔ5S (Fig. 3*D*).

Table 2 displays the structural differences between each of the progesterone sulfates tested. PMΔ5S and PM5S had similar agonistic properties and activated TRPM3 to the greatest degree. Structurally, they are similar in shape and are likely to bind to TRPM3 in similar ways. PM4S has some structural similarities to PM5S and PMΔ5S; the carbon 5 has the same orientation as PM5S, although the sulfate group is orientated in the α position (i.e., opposite to PMΔ5S and PM5S). The PM3S sulfate group is orientated in the α-direction compared with the β-orientation in PMΔ5S and PM5S. It is likely that the orientation of the carbon 5 and sulfate group is important for determining which progesterone sulfates can bind and activate TRPM3.

Computational Structure of TRPM3 and Modeling of Ligand Binding

Given the predicted 3D conformational differences between the different progesterone sulfates, we investigated how these differences affected binding to the TRPM3 receptor using computational modeling.

The final quality of the tetra-protomeric model of human TRPM3 (Supplementary Fig. 3), built through comparative modeling on the crystallographic solved structure of the mouse TRPM7 homolog (22), was carefully checked with the "Protein Geometry" program of the MOE "Protein" module. The Ramachandran plot of the final model showed a very good distribution of the φ and ψ angles, as reported in Supplementary Fig. 4.

Molecular docking results, shown in Supplementary Table 5, list the approximate binding free energy, expressed in kilocalories per mole, for all of the tested ligands on the three TRPM7 putative binding sites identified by cholesterol hemisuccinate in the study by Duan et al. (22). Our tested ligands, such as the progesterone sulfates PMΔ5S and PM5S, share the same cyclopentanoperhydrophenanthrene template scaffold of cholesterol, so structural data obtained from mouse TRPM7 are exploitable for our purposes. A detailed analysis of the docking poses generated in the three human TRPM3 binding sites allowed us to disregard poses that do not share the same binding mode of cholesterol hemisuccinate, scoring the remaining ones according to their binding free energy values.

Figure 4 depicts cholesterol hemisuccinate binding modes at its three binding sites; Fig. 5 shows how cholesterol hemisuccinate interacts with the amino acid residues on TRPM7 at each of its sites. Fig. 6 displays cholesterol hemisuccinate superimposed on PM5S at all three sites. The first two sites, displayed in Fig. 6*A* and *B*, show the similar binding position both ligands can achieve. However, Fig. 6*C* shows that site 3 has no suitable position for superimposition. Supplementary Figure 5 shows that progesterone sulfates share a very similar binding mode to cholesterol hemisuccinate when docked in two of the three available binding sites. However, for the third site, progesterone sulfate does not show the same binding mode when compared with the arrangement of cholesterol hemisuccinate. Supplementary Figure 6 displays the similarities in progesterone sulfate interactions to both of its two identified binding sites. Cholesterol hemisuccinate, PMΔ5S, and PM5S have similar amino acid residue interactions at both sites. The most notable shared amino acid interactions at site 1 were methionine, lysine, and tyrosine, with a set of hydrogen bonds formed between ligands and the active sites; in contrast, asparagine and tryptophan are the most notable shared amino acid interactions at site 2. Supplementary Table 5 suggests that PM3S has a very low binding affinity and binding mode for all of the three tested sites. This result corroborates our observation that PM3S is unable to stimulate calcium release in TRPM3-expressing HEK293 cells. The conformation of PMΔ5S and PM5S superimposes well on that of cholesterol hemisuccinate, and our data suggest that they will bind at two out of three sites on our comparative model of TRPM3, supporting our observation that PMΔ5S and PM5S stimulate TRPM3-mediated calcium release.

DISCUSSION

We have shown that serum concentrations of the sulfated progesterone metabolites PM5S, PM3S, and PMΔ5S are lowered in the third trimester of pregnancy in women with GDM and that PM3S is reduced in women of European ancestry with GDM and a BMI >30 kg/m^2. PM5S was also decreased in first trimester serum samples from women with BMI ≥35 kg/m^2 and no previously known impairment in glucose tolerance who were diagnosed with GDM in later pregnancy. PM5S, consistently lowered in each cohort, was demonstrated to augment GSIS in both mouse and human islets at high glucose concentrations. This effect was abolished using the well-established TRPM3 antagonist ISO (26), but not in *Tgr5*$^{-/-}$ or *Fxr*$^{-/-}$ mouse islets, suggesting the PM5S-associated increase in GSIS is mediated through TRPM3. PM5S administration also caused concentration-dependent increases in intracellular calcium concentration in TRPM3-transfected HEK cells, similar to PMΔ5S, a known agonist of TRPM3 (14) that is also reduced in the serum of women with GDM. Thus, lower levels of serum PM5S may contribute to impaired glucose homeostasis in women with GDM.

To date, no research has been conducted on serum concentrations of progesterone sulfates in GDM pregnancies. Of note, in the first trimester only, women with a BMI ≥35 kg/m^2 who subsequently developed GDM had lower serum concentrations of PM5S. BMI has been used as a predictor for GDM, with higher BMI associated with increased susceptibility to developing GDM (27–29). Examining progesterone sulfates in different BMI ranges could also show differences in concentrations and possibly be used as an

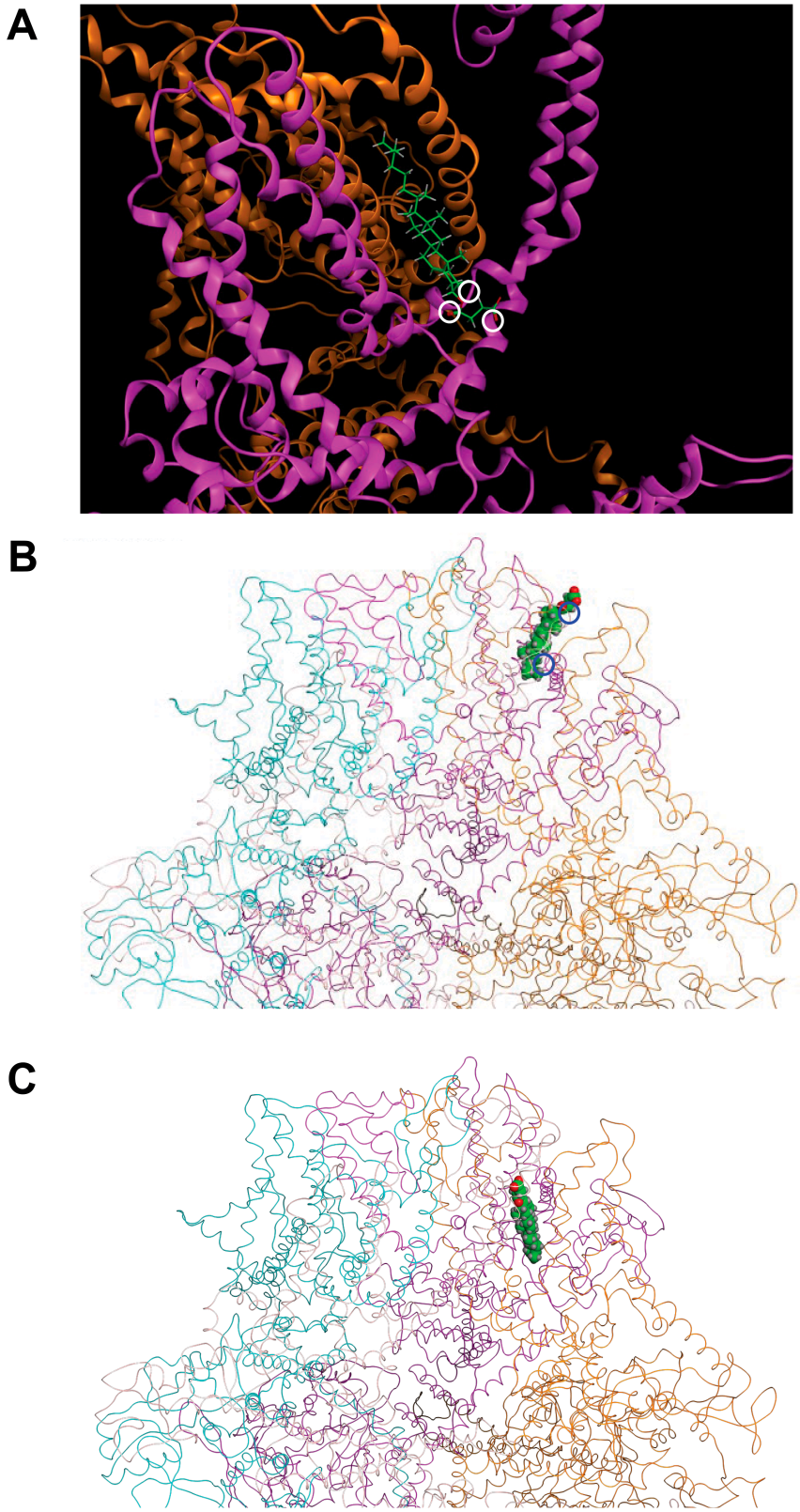

Figure 4—Cholesterol hemisuccinate binding. Cholesterol hemisuccinate binding to three sites on TRPM3. The 3D structure of cholesterol hemisuccinate binding at the first site (white circles indicate the key amino acid residues interacting with the ligand according to Fig. 5) (*A*), at the second site (blue circles indicate key amino acid residues interacting with the ligand according to Fig. 5) (*B*), and at the third site (*C*).

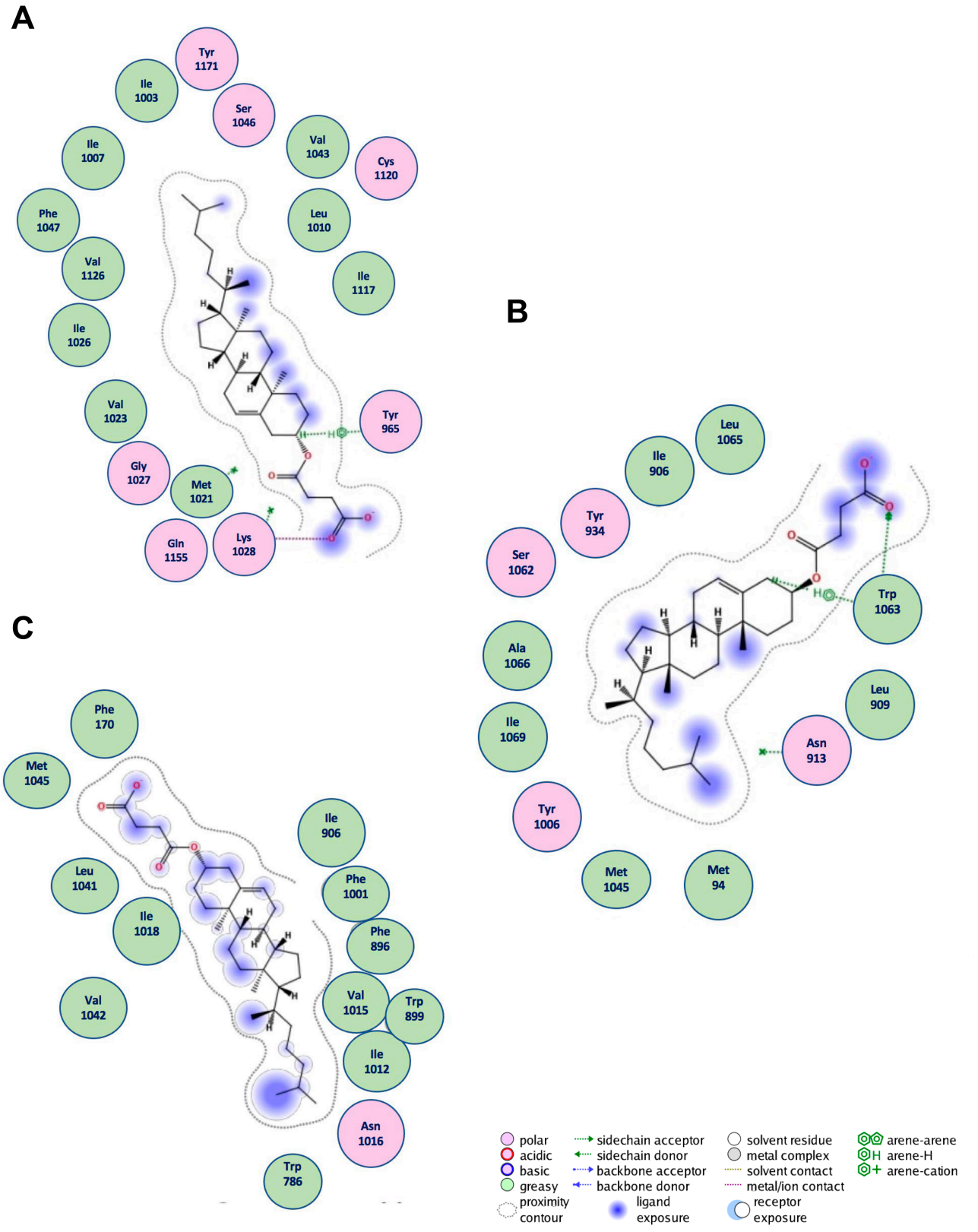

Figure 5—Amino acid–ligand binding site interaction. Cholesterol hemisuccinate showing the amino acid interactions at site 1 (*A*), site 2 (*B*), and site 3 (*C*).

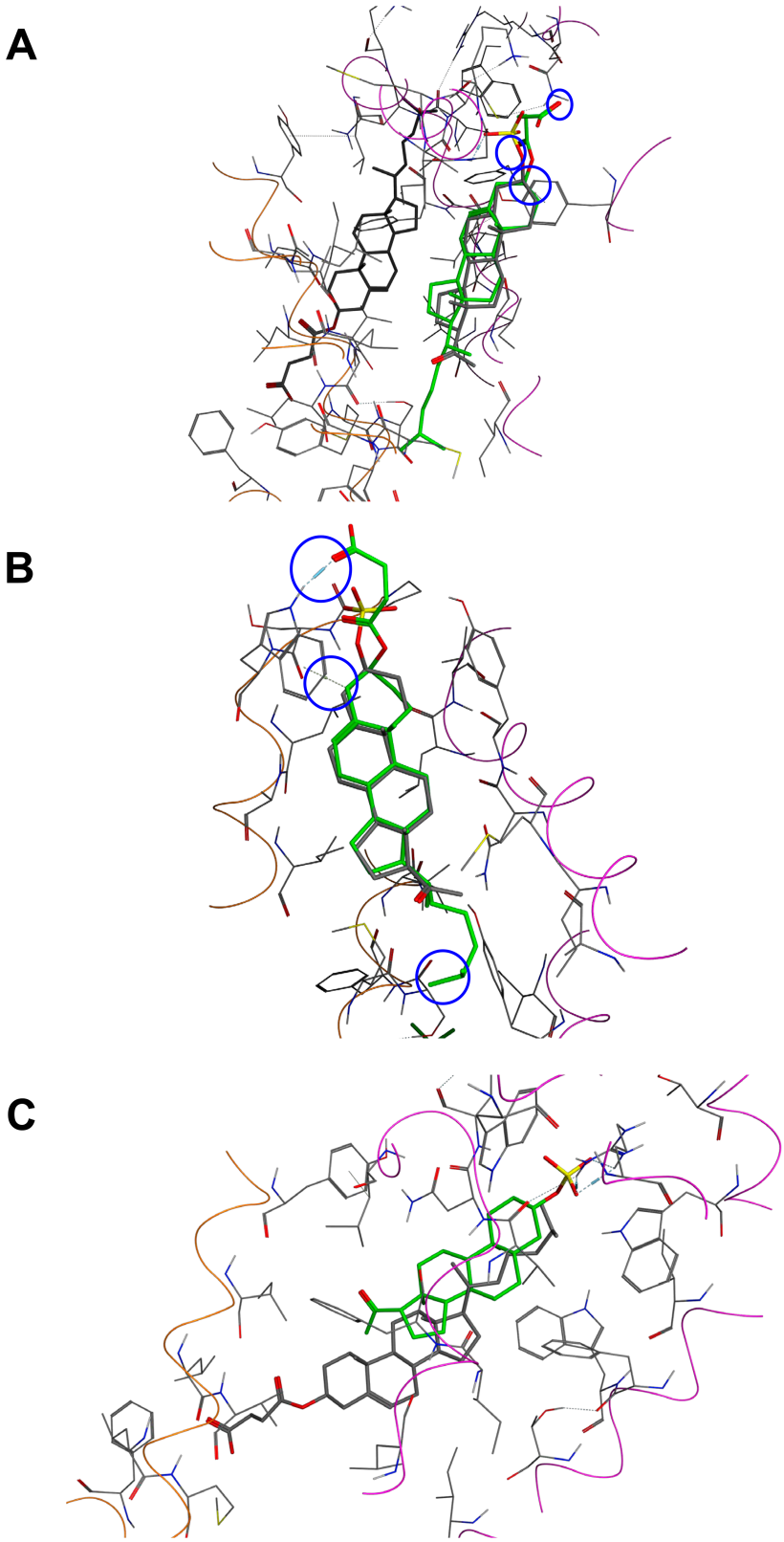

Figure 6—Ligand superimposition at each binding site. PM5S (shown in gray) showing good superimposition in *A* and *B* on top of the cholesterol hemisuccinate ligand (shown in green) binding displayed at sites 1 and 2, respectively. *C* shows cholesterol hemisuccinate (shown in gray), with no suitable pose for superimposition of PM5S (shown in green) at site 3. Blue circles indicate key interactions of the ligand binding to amino acids according to Fig. 5.

indicator of the concentration range in women with GDM. Cohort 3 demonstrated some differences between obese and normal BMI in the third trimester. Women with an obese BMI had a significant difference in PM3S concentrations between women without GDM and with GDM, which was not seen in women with a normal BMI. Future GDM studies examining progesterone sulfates should differentiate patient cohorts by BMI to ensure differences are related to GDM status and not BMI. Cohort 1 had significant differences in multiple progesterone sulfate concentrations that were not seen in the other cohorts. We speculate this may be due to ethnicity differences, and the differences with cohort 4 may be due to samples in this cohort being from the first trimester, whereas the other cohorts used samples that were taken at a later stage of pregnancy. It will be of interest for future studies to compare women of different ethnicities with GDM.

We next investigated how progesterone sulfates interact with the islets of Langerhans to modulate glucose homeostasis. Our results suggest that PM5S plays a role in the increased GSIS that occurs during normal pregnancy. Lower levels of PM5S in pre-GDM and GDM pregnancies might contribute to the reduction of insulin secretion in GDM (30), and decreased PM5S in the first trimester may similarly promote GDM development by reduced insulin secretion.

Previous work has established that islets express TRPM3 and that activation by the progesterone sulfate PMΔ5S causes insulin secretion (14,15). We have extended this observation to demonstrate that progesterone metabolites with a sulfate group at the carbon-3 of the steroid ring in the β-position are able to activate TRPM3 and induce GSIS in islets. Structurally, PMΔ5S and PM5S are very similar, and PM5S meets most of the reported structural requirements to activate TRPM3 as established previously (13,31). The TRPM3 antagonist ISO abolished the PM5S-induced increase in GSIS, consistent with PM5S acting via TRPM3; this was further supported by the increase in intracellular calcium in TRPM3-expressing HEK293 cells incubated with PM5S. This was similar to a study that demonstrated a single concentration (50 μmol/L) of PM5S or PMΔ5S almost equally activated TRPM3-transfected HEK293 cells (13), consistent with our findings of PM5S-induced GSIS in islets. Furthermore, a recent study using the insulin-releasing cell line INS-1 showed that PMΔ5S (100 μmol/L) can activate TRPM3, increasing GSIS and allowing calcium entry into the cell. TRPM3-deficient INS-1 cells also had reduced PMΔ5S-induced GSIS as well as lacking PMΔ5S-induced calcium signals (32), further supporting our results. It is intriguing that a previous study of pregnant *Tgr5*$^{-/-}$ and *Fxr*$^{-/-}$ mice demonstrated impaired insulin release in vivo, whereas the ex vivo islet studies reported in this article did not show impaired insulin secretion (12). It is possible that there are whole-body differences and compensatory mechanisms in the *Tgr5*$^{-/-}$ and *Fxr*$^{-/-}$ mice that are not replicated using direct islet stimulations. Also, as islets from nonpregnant female mice were studied, we could not establish whether islets isolated from pregnant mice would respond differently to progesterone sulfates compared to islets from nonpregnant female mice.

Currently, no high-resolution 3D crystal structure of TRPM3 has been solved. Our homology model of TRPM3 was computed to help predict how and where progesterone sulfate derivatives bind to the channel. This reveals further information on potential TRPM3 regulation mechanisms occurring at the cellular membrane and gives a molecular representation of how progesterone sulfate metabolites could bind TRPM3.

Since our template is based on mouse TRPM7, we used ligand binding models of cholesterol hemisuccinate to TRPM7 to predict how progesterone sulfates would bind to the active site of human TRPM3. TRPM3 channels have some similarities to TRPM7 (e.g., both are highly permeable to calcium ions) (33). The biophysical properties of TRPM3 and TRPM7 are similar, and their primary structures show high similarity level and well-conserved secondary structure features (34). Deciphering the TRPM3 ligand binding mode is important to further understand the function of this channel. Our results suggest that, among the tested ligands, similar amino acid interactions are involved in two out of three of the investigated binding sites and are therefore likely to operate this target in a similar way. Few studies have investigated TRPM3 ligand binding complexes. A recent study constructed crystal structures of Gβγ-proteins complexed with TRPM3 and confirmed the Gβγ-protein binding with the specific exon 17–encoded peptide in TRPM3 through mutagenesis experiments (35). Our structural bioinformatics approach can help predict the affinity and the binding modes when ligands are complexed to their receptor. Knowing how progesterone sulfates can specifically interact with TRPM3 is a key step in understanding the multifaceted biological activities of these molecules.

Progesterone sulfates could have nonislet targets. Previous work has shown that these steroid molecules are ligands for the bile acid receptors FXR and TGR5 and that molecules with different sulfated moieties signal with variable potency (10,11). The impact of progesterone sulfate signaling in hepatocytes, enterocytes, L-cells, and adipocytes would be a valuable focus for future studies. Like bile acids, progesterone sulfates may be generated and modified in the hepatocyte and small intestine (36). The sulfation process is normally a detoxification and regulation pathway and has been assumed to eliminate the active form of progesterone. It is noteworthy that PM3S and PM4S did not enhance GSIS from islets, and they did not evoke the same magnitude of calcium response as seen with PM5S or PMΔ5S in TRPM3-transfected HEK293T cells. Thus, the orientation of the sulfate moieties in different progesterone sulfates may influence their roles in glucose and lipid homeostasis and could play a role in susceptibility to other gestational diseases. For example, higher concentrations of PM5S have been found in women diagnosed with intrahepatic cholestasis of

pregnancy (10). It will be of interest for future studies to focus on the site and regulation of sulfation of specific progesterone metabolites.

Progesterone can influence insulin resistance (37), so it is possible sulfated progesterone metabolites have a similar effect. At present, there are conflicting reports about serum progesterone concentrations in GDM, with some studies reporting higher concentrations (37–39) and progesterone being noted to inhibit insulin secretion (40). However, others report no difference compared with uncomplicated pregnancy (41–43).

In this study, we have identified reduced serum progesterone sulfates in pregnancies complicated by GDM and have shown that serum PM5S concentrations are already reduced in the first trimester prior to GDM onset in women with a high BMI. PM5S is a strong activator of TRPM3 and augmented GSIS in both mouse and human islets. Lower serum concentrations of progesterone sulfates in pregnancies with GDM could reduce the level of insulin released in response to high serum glucose and therefore contribute to glucose intolerance during pregnancy. Together, these results indicate a link among progesterone sulfates, insulin secretion, and the development of GDM, particularly in women of European ancestry.

Acknowledgments. The authors thank Kristina Schoonjans, École Polytechnique Fédérale de Lausanne, Lausanne, Switzerland, for providing the *Fxr*$^{-/-}$ and *Tgr5*$^{-/-}$ knockout mice.

Funding. This research is funded by Tommy's Charity, the Fetal Medicine Foundation, the Lauren Page Trust, the John Coates Charitable Trust and the National Institute for Health Research (NIHR) Biomedical Research Centres at Guy's and St Thomas' NHS Foundation Trust and King's College London (IS-BRC-1215-20006). C.W. is funded by an NIHR Senior Investigator award.

The views expressed are those of the authors and not necessarily those of the National Health Service, NIHR, or the Department of Health.

Duality of Interest. No potential conflicts of interest relevant to this article were reported.

Author Contributions. C.W. conceived the study. A.L.M., G.A.B., and C.W. coordinated the collaborative studies. H.M.F. conducted the laboratory experiments, analyzed the data, and wrote the manuscript with overall supervision from A.L.M. and C.W. E.B. designed and conducted the *Fxr*$^{-/-}$ and *Tgr5*$^{-/-}$ islet experiments. S.M., P.J., and J.E.B. assisted with conducting and/or designing the islet experiments. D.M. provided the HAPO samples. K.F.H. provided the London GDM samples. A.S. and K.H.N. provided the early pregnancy samples. N.S., N.P., Y.W., and P.S. provided the data for the PRiDE study cohort. A.L.-S. and H.-U.M. assayed the human serum samples using UPLC-MS/MS. L.I.P., D.A., and S.B. were involved in designing and assisting in the calcium experiments. M.G., I.E., and F.F. designed and supervised the experiments to model the structure and ligand binding of TRPM3. P.T.S. assisted with the statistical analysis. All authors reviewed the data and contributed to writing the manuscript. C.W. is the guarantor of this work and, as such, had full access to all of the data in the study and takes responsibility for the integrity of the data and the accuracy of the data analysis.

References

1. Lee KW, Ching SM, Ramachandran V, et al. Prevalence and risk factors of gestational diabetes mellitus in Asia: a systematic review and meta-analysis. BMC Pregnancy Childbirth 2018;18:494

2. Feig DS, Hwee J, Shah BR, Booth GL, Bierman AS, Lipscombe LL. Trends in incidence of diabetes in pregnancy and serious perinatal outcomes: a large, population-based study in Ontario, Canada, 1996-2010. Diabetes Care 2014;37:1590–1596

3. White SL, Pasupathy D, Sattar N, et al.; UPBEAT Consortium. Metabolic profiling of gestational diabetes in obese women during pregnancy. Diabetologia 2017;60:1903–1912

4. Ryckman KK, Spracklen CN, Smith CJ, Robinson JG, Saftlas AF. Maternal lipid levels during pregnancy and gestational diabetes: A systematic review and meta-analysis. BJOG 2015;122:643–651

5. Tobias DK, Stuart JJ, Li S, et al. Association of history of gestational diabetes with long-term cardiovascular disease risk in a large prospective cohort of US women. JAMA Intern Med 2017;177:1735–1742

6. Ovesen PG, Jensen DM, Damm P, Rasmussen S, Kesmodel US. Maternal and neonatal outcomes in pregnancies complicated by gestational diabetes. a nation-wide study. J Matern Fetal Neonatal Med 2015;28:1720–1724

7. Metzger BE, Lowe LP, Dyer AR, et al.; HAPO Study Cooperative Research Group. Hyperglycemia and adverse pregnancy outcomes. N Engl J Med 2008;358:1991–2002

8. Bellamy L, Casas JP, Hingorani AD, Williams D. Type 2 diabetes mellitus after gestational diabetes: a systematic review and meta-analysis. Lancet 2009;373:1773–1779

9. Saravanan P; Diabetes in Pregnancy Working Group; Maternal Medicine Clinical Study Group; Royal College of Obstetricians and Gynaecologists, UK. Gestational diabetes: opportunities for improving maternal and child health. Lancet Diabetes Endocrinol 2020;8:793–800

10. Abu-Hayyeh S, Papacleovoulou G, Lövgren-Sandblom A, et al. Intrahepatic cholestasis of pregnancy levels of sulfated progesterone metabolites inhibit farnesoid X receptor resulting in a cholestatic phenotype. Hepatology 2013;57:716–726

11. Abu-Hayyeh S, Ovadia C, Lieu T, et al. Prognostic and mechanistic potential of progesterone sulfates in intrahepatic cholestasis of pregnancy and pruritus gravidarum. Hepatology 2016;63:1287–1298

12. Bellafante E, McIlvride S, Nikolova V, et al. Maternal glucose homeostasis is impaired in mouse models of gestational cholestasis. Sci Rep 2020;10:11523

13. Drews A, Mohr F, Rizun O, et al. Structural requirements of steroidal agonists of transient receptor potential melastatin 3 (TRPM3) cation channels. Br J Pharmacol 2014;171:1019–1032

14. Wagner TFJ, Loch S, Lambert S, et al. Transient receptor potential M3 channels are ionotropic steroid receptors in pancreatic β cells. Nat Cell Biol 2008;10:1421–1430

15. Thiel G, Müller I, Rössler OG. Signal transduction via TRPM3 channels in pancreatic β-cells. J Mol Endocrinol 2013;50:R75–R83

16. Bowe JE, Hill TG, Hunt KF, et al. A role for placental kisspeptin in β cell adaptation to pregnancy. JCI Insight 2019;4:e124540

17. Saravanan P, Sukumar N, Adaikalakoteswari A, et al. Association of maternal vitamin B 12 and folate levels in early pregnancy with gestational diabetes: a prospective UK cohort study (PRiDE study). Diabetologia 2021;64:2170–2182

18. Thomas C, Gioiello A, Noriega L, et al. TGR5-mediated bile acid sensing controls glucose homeostasis. Cell Metab 2009;10:167–177

19. Milona A, Owen BM, van Mil S, et al. The normal mechanisms of pregnancy-induced liver growth are not maintained in mice lacking the bile acid sensor Fxr. Am J Physiol Gastrointest Liver Physiol 2010;298:G151–G158

20. Huang GC, Zhao M, Jones P, et al. The development of new density gradient media for purifying human islets and islet-quality assessments. Transplantation 2004;77:143–145

21. Jones PM, Salmon DMW, Howell SL. Protein phosphorylation in electrically permeabilized islets of Langerhans. Effects of Ca2+, cyclic AMP, a phorbol ester and noradrenaline. Biochem J 1988;254:397–403

22. Duan J, Li Z, Li J, et al. Structure of the mammalian TRPM7, a magnesium channel required during embryonic development. Proc Natl Acad Sci USA 2018;115:E8201–E8210

23. Labute P. The generalized Born/volume integral implicit solvent model: estimation of the free energy of hydration using London dispersion instead of atomic surface area. J Comput Chem 2008;29:1693–1698
24. Naïm M, Bhat S, Rankin KN, et al. Solvated interaction energy (SIE) for scoring protein-ligand binding affinities. 1. Exploring the parameter space. J Chem Inf Model 2007;47:122–133
25. Kumar DP, Rajagopal S, Mahavadi S, et al. Activation of transmembrane bile acid receptor TGR5 stimulates insulin secretion in pancreatic β cells. Biochem Biophys Res Commun 2012;427:600–605
26. Straub I, Krügel U, Mohr F, et al. Flavanones that selectively inhibit TRPM3 attenuate thermal nociception in vivo. Mol Pharmacol 2013;84:736–750
27. Takmaz T, Yalvaç ES, Özcan P, Çoban U, Gökmen Karasu AF, Ünsal M. The predictive value of weight gain and waist circumference for gestational diabetes mellitus. Turk J Obstet Gynecol 2019;16:199–204
28. Zheng T, Ye W, Wang X, et al. A simple model to predict risk of gestational diabetes mellitus from 8 to 20 weeks of gestation in Chinese women. BMC Pregnancy Childbirth 2019;19:252
29. Artzi NS, Shilo S, Hadar E, et al. Prediction of gestational diabetes based on nationwide electronic health records. Nat Med 2020;26:71–76
30. Reddi Rani P, Begum J. Screening and diagnosis of gestational diabetes mellitus, where do we stand. J Clin Diagn Res 2016;10:QE01–QE04
31. Majeed Y, Agarwal AK, Naylor J, et al. Cis-isomerism and other chemical requirements of steroidal agonists and partial agonists acting at TRPM3 channels. Br J Pharmacol 2010;161:430–441
32. Becker A, Mannebach S, Mathar I, et al. Control of insulin release by transient receptor potential melastatin 3 (TRPM3) ion channels. Cell Physiol Biochem 2020;54:1115–1131
33. Huang Y, Fliegert R, Guse AH, Lü W, Du J. A structural overview of the ion channels of the TRPM family. Cell Calcium 2020;85:102111
34. Harteneck C. Function and pharmacology of TRPM cation channels. Naunyn Schmiedebergs Arch Pharmacol 2005;371:307–314
35. Behrendt M, Gruss F, Enzeroth R, et al. The structural basis for an on-off switch controlling Gβγ-mediated inhibition of TRPM3 channels. Proc Natl Acad Sci USA 2020;117:29090–29100
36. Alnouti Y. Bile acid sulfation: a pathway of bile acid elimination and detoxification. Toxicol Sci 2009;108:225–246
37. Brănişteanu DD, Mathieu C. Progesterone in gestational diabetes mellitus: guilty or not guilty? Trends Endocrinol Metab 2003;14:54–56
38. Park S, Kim MY, Baik SH, et al. Gestational diabetes is associated with high energy and saturated fat intakes and with low plasma visfatin and adiponectin levels independent of prepregnancy BMI. Eur J Clin Nutr 2013;67:196–201
39. Couch SC, Philipson EH, Bendel RB, Pujda LM, Milvae RA, Lammi-Keefe CJ. Elevated lipoprotein lipids and gestational hormones in women with diet-treated gestational diabetes mellitus compared to healthy pregnant controls. J Diabetes Complications 1998;12:1–9
40. Straub SG, Sharp GW, Meglasson MD, De Souza CJ. Progesterone inhibits insulin secretion by a membrane delimited, non-genomic action. Biosci Rep 2001;21:653–666
41. Li M, Song Y, Rawal S, et al. Plasma prolactin and progesterone levels and the risk of gestational diabetes: a prospective and longi-tudinal study in a multiracial cohort. Front Endocrinol (Lausanne) 2020;11:83
42. Grigorakis SI, Alevizaki M, Beis C, Anastasiou E, Alevizaki CC, Souvatzoglou A. Hormonal parameters in gestational diabetes mellitus during the third trimester: high glucagon levels. Gynecol Obstet Invest 2000;49:106–109
43. Todoric J, Handisurya A, Perkmann T, et al. Circulating progranulin levels in women with gestational diabetes mellitus and healthy controls during and after pregnancy. Eur J Endocrinol 2012;167:561–567